*J. Phys. Chem Solids* Pergamon Press 1967. Vol. 28, pp. 439–447. Printed in Great Britain.

# ELASTIC CONSTANTS AND CALCULATED LATTICE VIBRATION FREQUENCIES OF $Mg_2Sn$*

**L. C. DAVIS,† W. B. WHITTEN‡ and G. C. DANIELSON**

Institute for Atomic Research and Department of Physics,
Iowa State University, Ames, Iowa, U.S.A.

(*Received* 8 *August* 1966)

**Abstract**—The longitudinal and shear sound velocities of $Mg_2Sn$ in the [100], [110] and [111] directions have been measured between 80 and 300°K by a resonance technique. The elastic constants were computed from these velocities. Lattice vibration frequencies have been calculated for two point ion models and a shell model. Best agreement with the experimental specific heat data was obtained for the shell model, which reproduced quite accurately the sharp minimum in the Debye temperature near 20°K.

## INTRODUCTION

$Mg_2Sn$ is a II–IV compound semiconductor with the fluorite structure and is a member of the family of compounds $Mg_2X$, where $X$ can be Si, Ge, Sn, or Pb. The elastic constants and calculated lattice vibration frequencies have been reported for $Mg_2Si$ by Whitten *et al.*[1] and for $Mg_2Ge$ by Chung *et al.*[2] The present investigation was undertaken to extend our knowledge of the elastic properties of the $Mg_2X$ family to include $Mg_2Sn$.

The reststrahl frequency and high and low frequency dielectric constants of $Mg_2Sn$ have been measured by Kahan *et al.*[3] Just as in the cases of $Mg_2Si$[1] and $Mg_2Ge$,[2] it seemed feasible to calculate the lattice vibration frequencies from these optical constants and the elastic constants which we could measure. In addition to the two point ion models described by Chung *et al.*,[2] a new model which takes into account the polarizability of the Sn ions can be used. The calculated specific heat of the three models can then be compared to the experimental data of Jelinek *et al.*[4]

The phonon dispersion curves are important for an interpretation of the semiconducting properties of these compounds.[5–7] Piezoresistance measurements have shown that the energy minima lie along the ⟨100⟩ axes in $Mg_2Si$[8] and in $Mg_2Sn$.[9] Therefore, a knowledge of the phonon frequencies in the ⟨100⟩ directions is particularly important since such phonons are involved in indirect transitions between the valence band and the conduction band.

## EXPERIMENTAL SOUND VELOCITIES AND ELASTIC CONSTANTS

The velocity of sound in $Mg_2Sn$ was measured by a resonance technique. Two 10 MHz quartz transducers were bonded to opposite parallel faces on each sample. One transducer was driven by the output from an Arenberg ultrasonic oscillator, Model PG-650C, operating in the continuous wave mode. The output of the other transducer was amplified and displayed on a scope. Frequencies were measured with a Bolton Labs BC-221-AL frequency meter. The sample holder is shown in Fig. 1. Two different materials were used to bond the transducers to the sample: below 250°K, vacuum grease was used; and above 250°K, beeswax was used.

Single crystal ingots were grown by a Bridgman method. Three samples were prepared with orientations [100], [110], and [111]. The sample lengths were 0·520, 0·375 and 0·943 cm, respectively.

* Work was performed in the Ames Laboratory of the U.S. Atomic Energy Commission. Contribution No. 1943.

† AEC Postdoctoral Fellow.

‡ Now at Brookhaven National Laboratory, Upton, N.Y., U.S.A.

Parallel faces on opposite ends of each sample were polished with diamond paste on a silk velvet cloth. It was found that polished faces were necessary in order to obtain clear resonances.

As the frequency of the oscillator was swept from 5 to 15 MHz, 15–25 resonances could be detected. The condition for a resonance has been given by WILLIAMS and LAMB[10] as:

$$2\pi f_n \tau - \phi_n = n\pi,$$

where $\tau = l/v$, $l$ is the sample length and $v$ is the velocity of sound, $f_n$ is the resonant frequency and

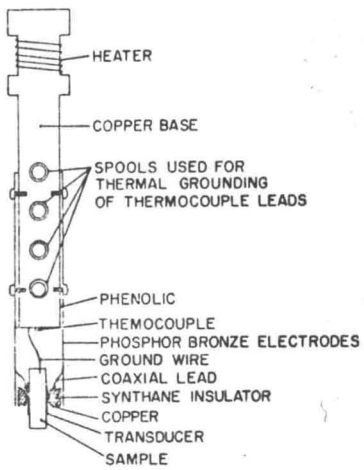


FIG. 1. Sample holder for sound velocity measurements.

$\phi_n$ is the phase shift which occurs when a sound wave is reflected at the sample boundary. WILLIAMS and LAMB[10] have derived an expression for $\phi_n$ as a function of frequency, depending upon the acoustic impedances of the sample, bonding material, and transducers, and upon the resonant frequency of the transducers (10 MHz in this case). However, it was found experimentally that for $Mg_2Sn$, $\phi_n$ was nearly frequency independent except near 10 MHz where we expected a phase shift of 180° as the frequency was passed through the fundamental of the transducers.

In the region where $\phi_n$ is independent of frequency, the velocity of sound is given by:

$$v = 2l\frac{df_n}{dn}$$

As a check, measurements were made of the velocity of sound in Ge and compared to the values of MCSKIMMIN.[11] It was found that shear measurements agreed to within 1 percent and longitudinal measurements to within 2 percent over the temperature range 77–300°K.

The velocity of sound in $Mg_2Sn$ is shown in Figs. 2 and 3. The solid lines in Fig. 3 were computed from the three velocities in Fig. 2, and agreed satisfactorily with the measured values. None of the velocities showed more than a 2·5 percent change between 100° and 300°K. From the sound velocities and the X-ray density of

$$3{\cdot}592\ \mathrm{g/cm^3},^{(12)}$$

the elastic constants at 300°K were calculated to be:

$$C_{11} = (8{\cdot}24 \pm 0{\cdot}33) \times 10^{11}\ \mathrm{dyn/cm^2},$$
$$C_{12} = (2{\cdot}08 \pm 0{\cdot}33) \times 10^{11}\ \mathrm{dyn/cm^2},$$
$$C_{44} = (3{\cdot}66 \pm 0{\cdot}07) \times 10^{11}\ \mathrm{dyn/cm^2}.$$

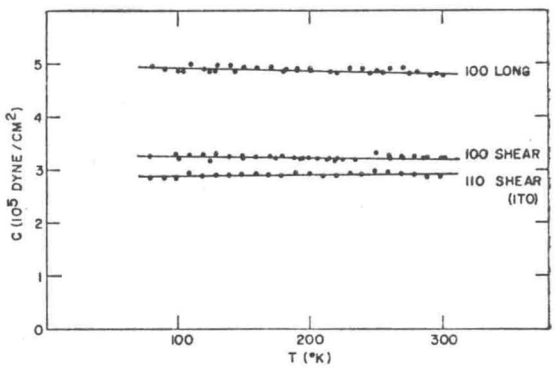


FIG. 2. Sound velocity in $Mg_2Sn$: [100] and [110] directions.

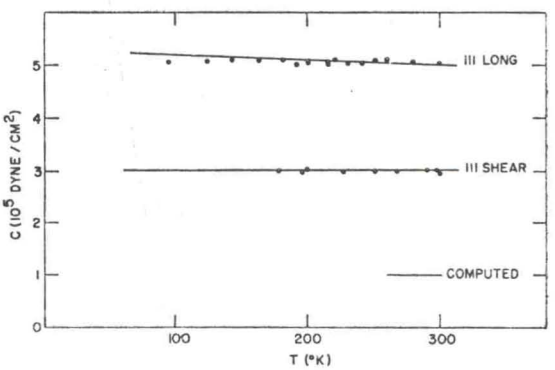


FIG. 3. Sound velocity in $Mg_2Sn$: [111] direction. Solid line computed from the three velocities in Fig. 2.

The isotropy coefficient, $S = (C_{11}-C_{12})/2C_{44}$, which has the value 1 for an isotropic crystal, was found to be 0·84 for $Mg_2Sn$. The temperature dependence of the elastic constants is shown in Fig. 4. Sample lengths and densities were corrected for thermal expansion using the coefficient of linear expansion which was determined by

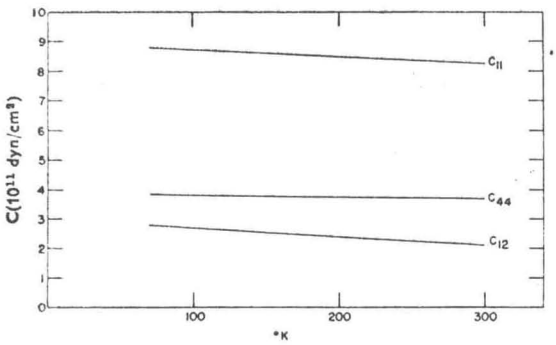


FIG. 4. Elastic constants of $Mg_2Sn$.

SHANKS.[13] He obtained a value of $0{\cdot}99\times10^{-5}/°K$ from the temperature dependence of the lattice constant as measured from X-ray diffraction patterns.

Listed in Table 1 are the elastic constants for a number of common semiconductors. It should be noted that $Mg_2Sn$ is somewhat different from the related compounds $Mg_2Si$ and $Mg_2Ge$. The elastic constants, especially $C_{11}$, are smaller, and $Mg_2Sn$ is less isotropic than either $Mg_2Si$ or $Mg_2Ge$. A similar reduction in the values of the elastic constants can be seen in a comparison of GaAs and GaSb and of InAs and InSb. In fact, the elastic constants of $Mg_2Sn$ resemble those of GaSb except that $C_{12}$ is only about one-half of $C_{44}$ in $Mg_2Sn$. The relative magnitudes of the elastic constants, $C_{11} > C_{44} > C_{12}$, are the same as in Si and Ge. The $Mg_2X$ compounds are more isotropic than any of the other semiconductors listed.

## INTERATOMIC FORCE MODELS

KAHAN *et al.*[3] have measured the high and low frequency dielectric constants, $\epsilon_\infty$ and $\epsilon_0$, and the reststrahl (transverse optic) frequency $\omega_{IT}$ for $Mg_2Sn$. They found $\epsilon_\infty = 15{\cdot}5$, $\epsilon_0 = 23{\cdot}75$, and $\omega_{IT} = 3{\cdot}50\times10^{13}\ \text{sec}^{-1}$. From the LYDDANE–SACHS–TELLER[16] relation,

$$\frac{\omega_{IL}}{\omega_{IT}} = \sqrt{\left(\frac{\epsilon_0}{\epsilon_\infty}\right)},$$

we found the longitudinal optic frequency, $\omega_{IL}$, to have the value $4{\cdot}33\times10^{3}\ \text{sec}^{-1}$.

*Table 1. Elastic constants of some common semiconductors*

| | $C_{11}$ (10 in. dyn/cm²) | $C_{12}$ | $C_{44}$ | $S=\dfrac{C_{11}-C_{12}}{2C_{44}}$ |
|---|---|---|---|---|
| $Mg_2Si$* | 12·1 | 2·2 | 4·64 | 1·07 |
| $Mg_2Ge$† | 11·79 | 2·30 | 4·65 | 1·02 |
| $Mg_2Sn$‡ | 8·24 | 2·08 | 3·66 | 0·84 |
| Si§ | 16·57 | 6·39 | 7·95 | 0·64 |
| Ge§ | 12·88 | 4·83 | 6·71 | 0·60 |
| GaAs‖ | 11·92 | 5·97 | 5·38 | 0·55 |
| GaSb‖ | 8·85 | 4·04 | 4·33 | 0·56 |
| InAs‖ | 8·33 | 4·53 | 3·96 | 0·48 |
| InSb‖ | 6·75 | 3·47 | 3·16 | 0·52 |

* Ref. 1.
† Ref. 2.
‡ Present investigation.
§ Ref. 14.
‖ Ref. 15.

From our measurements of the elastic constants and the above optical constants, it appeared feasible to make a calculation of the phonon dispersion curves for $Mg_2Sn$. Three different force constant models were employed in our calculation. The first two, model I and model II, were point ion models, previously proposed by WHITTEN *et al.*[1] and CHUNG *et al.*[2] for $Mg_2Si$ and $Mg_2Ge$. Models I and II differed only in the assumptions made concerning the short range forces between next nearest neighbors. The third model was a slight modification of the shell model as first proposed by DICK and OVERHAUSER[17] and successfully used by many authors.[18] Although few tests of the validity of our calculated phonon dispersion curves are currently available, it is clear that the shell model provided the best fit to the Debye curve as a function of temperature (see Fig. 5).

To construct a physically plausible picture of $Mg_2Sn$, apparently one must account for both an ionic character and a covalent character. The infrared reflectivity spectrum of $Mg_2Sn$ is characteristic of an ionic compound. The difference in

the high and low frequency dielectric constants is also characteristic of an ionic compound.

The relative sizes of the elastic constants $C_{44}$ and $C_{12}$, however, resemble those of covalent semiconductors. In fact, MOOSER and PEARSON[19] have suggested that covalent bonding is necessary for $Mg_2Sn$ to be a semiconductor. In addition, the small energy gap, 0·33 eV,[20] would indicate that $Mg_2Sn$ is not strongly ionic. Experimentally, model was the polarizable Sn ion (that is, a shell isotropically and harmonically bound to an Sn ion core). The polarizability of the lighter Mg ions was neglected.

We modified the usual shell model[17,18] slightly in that we did not include a force between the positive ion (Mg) and the Sn shell, but we did include a force between the Mg ion and the Sn core. Attempts to include a Mg ion–Sn shell force,

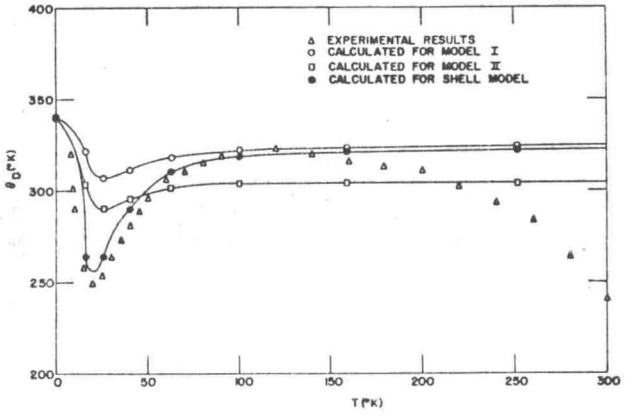


FIG. 5. The Debye temperature of $Mg_2Sn$ is shown as a function of temperature. Models I and II are point ion models. Best agreement with the experimental curve was obtained for the shell model which reproduced quite accurately the sharp minimum near 20°K. The decrease in the experimental curve above 140°K is probably due to anharmonic effects.

LICHTER[21] has concluded that the bonding in $Mg_2Sn$ is predominantly covalent from an investigation of the growth of $Mg_2Sn$ crystals from non-stoichometric melts. Therefore, we have taken $Mg_2Sn$ to be partially ionic and partially covalent.

The three force constant models we have used all contained long range Coulomb forces arising from the ionic charges and short range forces between nearest neighbors resulting from the covalent bonds. The short range forces of model I can be described by nearest neighbor Mg–Sn forces, both central and non-central, and second nearest neighbor Mg–Mg and Sn–Sn forces, only central. Model II had central and non-central Mg–Sn forces, central and non-central Sn–Sn forces, and no Mg–Mg force at all. The shell model had central and non-central forces between Mg–Sn ions and Sn–Sn ions, with a small central Mg–Mg force. The salient feature of the shell corresponding to the deformation dipole moment of KARO and HARDY,[22] gave poor agreement with the specific heat data. There may be some theoretical justification for neglecting the deformation dipole moment in $Mg_2Sn$. In an alkali halide, it is clear that the electronic distributions about the positive and negative ions repel one another when the ions are displaced from equilibrium and brought closer together. The repulsion of the electronic charge clouds gives rise to a deformation dipole moment. But when a substantial amount of covalent bonding is present (as in $Mg_2Sn$), it is not clear what the electronic distributions do, and it may be that the deformation dipole moments are small.

## DYNAMICS OF THE SHELL MODEL

We shall discuss only the dynamics of the shell model. The dynamics of the point ion models

which are quite similar to the shell model have been discussed in detail.[1,2]

The crystal structure of $Mg_2Sn$ is the same as $CaF_2$. (See Fig. 6.) The lattice is face-centered cubic and the basis consists of a Sn ion at the origin and Mg ions at $(a/4, a/4, a/4)$ and at $(\frac{3}{4}a, \frac{3}{4}a, \frac{3}{4}a)$, $a$ is the lattice constant. The Sn ions occupy centers of inversion symmetry, but Mg ions do not.

The lattice vibration frequencies are roots of the secular equation

$$|m_k\omega^2\delta_{kk'}\delta_{\alpha\beta}+[{}^{kk'}_{\alpha\beta}]| = 0, \qquad (1)$$

where $k = 1$ for the Sn core, $k = 1'$ for the Sn shell, and $k = 2$ and 4 for the Mg ions. $\alpha$ and $\beta$ index the coordinates $x$, $y$, and $z$. The coupling coefficients $[{}^{kk'}_{\alpha\beta}]$ are written as the sum of the short range and Coulomb coupling coefficients, $S[{}^{kk'}_{\alpha\beta}]$ and $C[{}^{kk'}_{\alpha\beta}]$. The Coulomb terms have been tabulated by KELLERMAN[23] and by WHITTEN *et al.*[1] for 47 points in the Brillouin zone. The only difference between $C[{}^{1k}_{\alpha\beta}]$ and $C[{}^{1k'}_{\alpha\beta}]$ is the charge multiplying the coefficient.

We list below the expression of GANESAN and SRINIVASAN[24] for the short range coupling coefficients with appropriate changes for our shell model.

$$S[{}^{11}_{\alpha\alpha}] = -8\alpha_1-4\alpha_2-8\beta_2+4\alpha_2\cos\frac{a}{2}q_\beta\cos\frac{a}{2}q_\gamma + 4\beta_2\cos\frac{a}{2}q_\alpha\left(\cos\frac{a}{2}q_\beta+\cos\frac{a}{2}q_\gamma\right)-\delta, \qquad (2)$$

$$S[{}^{11}_{\alpha\beta}] = 4\gamma_2\sin\frac{a}{2}q_\alpha\sin\frac{a}{2}q_\beta,$$

$$S[{}^{11'}_{\alpha\alpha}] = \delta,$$

$$S[{}^{11'}_{\alpha\alpha}] = 0,$$

$$S[{}^{12}_{\alpha\alpha}] = \alpha_1[\exp[i(a/4)(q_\alpha+q_\beta+q_\gamma)] + \exp[i(a/4)(q_\alpha-q_\beta-q_\gamma)] + \exp[i(a/4)(-q_\alpha+q_\beta-q_\gamma)] + \exp[i(a/4)(-q_\alpha-q_\beta+q_\gamma)]],$$

$$S[{}^{12}_{\alpha\beta}] = \beta_1[\exp[i(a/4)(q_\alpha+q_\beta+q_\gamma)] - \exp[i(a/4)(q_\alpha-q_\beta-q_\gamma)] - \exp[i(a/4)(-q_\alpha+q_\beta-q_\gamma)] + \exp[i(a/4)(-q_\alpha-q_\beta+q_\gamma)]],$$

$$S[{}^{1'2}_{\alpha\alpha}] = 0,$$

$$S[{}^{1'2}_{\alpha\beta}] = 0,$$

$$S[{}^{1'4}_{\alpha\alpha}] = 0,$$

$$S[{}^{1'4}_{\alpha\beta}] = 0,$$

$$S[{}^{22}_{\alpha\alpha}] = -4\alpha_1-2\alpha_3-4\beta_3,$$

$$S[{}^{22}_{\alpha\beta}] = 0,$$

$$S[{}^{24}_{\alpha\alpha}] = 2\beta_3\left(\cos\frac{a}{2}q_\beta+\cos\frac{a}{2}q_\gamma\right)+2\alpha_3\cos\frac{a}{2}q_\alpha,$$

$$S[{}^{24}_{\alpha\alpha}] = 0,$$

where $\alpha \neq \beta$ and $a$ is the lattice constant. The remaining coefficients can be obtained by the relations

$$S[{}^{kk'}_{\alpha\beta}] = S[{}^{k'k}_{\beta\alpha}]^*,$$
$$S[{}^{14}_{\alpha\beta}] = S[{}^{12}_{\alpha\beta}]^*. \qquad (3)$$

The subscripts 1, 2, and 3 on the force constants correspond to Mg–Sn, Sn–Sn, and Mg–Mg

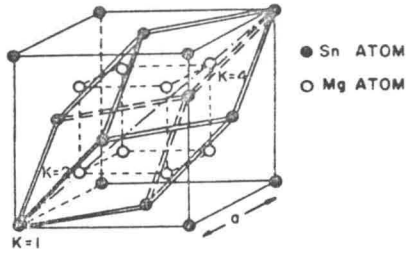


FIG. 6. The crystal structure of $Mg_2Sn$. The position vectors of the basis in the unit cell are given by $r_k = a/4(k-1)[1, 1, 1]$.

forces, respectively. $\delta$ is the force constant associated with the Sn core–Sn shell interaction. (See the appendix for exact definitions of force constants.)

In the limit of long wavelengths ($q = 0$), we have as roots of the secular equation:

$$\omega_A^2 = 0,$$

$$\omega_R^2 = \frac{4}{m_2}(\alpha_1+\alpha_2+2\beta_3),$$

$$\omega_I^2 = \left(\frac{2}{m_1}+\frac{1}{m_2}\right)\left(4\alpha_1-2C\frac{e_2^2}{V\left(1-\frac{4\pi}{3V}\alpha\right)}\right), \qquad (4)$$

where $C$ has the value $4\pi/3$ for transverse modes, $-8\pi/3$ for the longitudinal mode, $e_2$ is the charge on the Mg ions and in our shell model is equivalent to the SZIGETI[25,26] charge, $V$ is the volume of a primitive cell, $a^3/4$, and $\alpha = e_1'^2/\delta$ is the atomic polarizability of the Sn ion (where $e_1'$ is the charge on the Sn shell). $\alpha$ is related to the high frequency dielectric constant by

$$\frac{4\pi}{3V}\alpha = \frac{\epsilon_\infty - 1}{\epsilon_\infty + 2}. \tag{5}$$

For $Mg_2Sn$, we found $(4\pi/3V)\alpha = 0{\cdot}829$. In the point ion models, the expressions for the frequencies do not contain the $(4\pi/3V)\alpha$ term because the polarizability was neglected.

At the zone center, the acoustic modes, $\omega_A$, and the Raman modes, $\omega_R$, are triply degenerate, while the transverse infrared mode, $\omega_{IT}$, is doubly degenerate, and the longitudinal infrared mode, $\omega_{IL}$, is non-degenerate. Since $\omega_{IT}$ and $\omega_{IL}$ are known experimentally, the third expression in equation (4) can be used to evaluate $\alpha_1$ and $e_2$. (For numerical values of the shell model and the point ion models, see Table 2.) The Raman frequency is not known, so no information is gained from the second expression in equation (4).

*Table 2. Force constants (in units of* $10^4$ dyn/cm) *and* Mg *ion charge (in units of* $10^{-10}$ e.s.u.) *for various models*

| | $\alpha_1$ | $\beta_1$ | $\alpha_2$ | $\beta_2$ | $\alpha_3$ | $\beta_3$ | $e_2$ |
|---|---|---|---|---|---|---|---|
| Model I | 1·033 | 0·841 | 0 | 0·456 | 0·599 | 0 | 2·397 |
| Model II | 1·033 | 1·310 | 0·412 | 0·755 | 0 | 0 | 2·397 |
| Shell model | 1·290 | 1·365 | 0·356 | 0·567 | 0·250 | 0 | 1·630 |

The subscripts 1, 2 and 3 on the force constants correspond to Mg–Sn, Sn–Sn, and Mg–Mg forces respectively.

The polarization of the Sn ions will not affect the elastic constants since the Sn ions are at points of inversion symmetry. Therefore, we could take over the expressions given by CHUNG *et al.*[2] for the point ion models:

$$C_{11} = \frac{2}{a}\left(\alpha_1 + 2\beta_2 + \alpha_3 + 3{\cdot}276\frac{e_2^2}{V}\right),$$

$$C_{12} = \frac{2}{a}\left(2\beta_1 - 2\gamma_2 - \alpha_1 - \alpha_2 - \beta_2 - \beta_3 - 5{\cdot}395\frac{e_2^2}{V}\right), \tag{6}$$

$$C_{44} = \frac{2}{a}\left(\alpha_1 + \alpha_2 + \beta_2 + \beta_3 - 1{\cdot}527\frac{e_2^2}{V} - \frac{\left(-\beta_1 + 5{\cdot}038\frac{e_2^2}{V}\right)^2}{\alpha_1 + \alpha_3 + 2\beta_3}\right).$$

Following CHUNG *et al.*[2], we eliminated a disposable parameter by imposing axial symmetry about the line joining the two Sn ions, so that $\alpha_2 = \beta_2 + \gamma_2$. But equations (4), (5) and (6) did not uniquely define all the parameters in our shell model. In particular, equation (5) only determined the ratio $e_1'^2/\delta$. Therefore, we picked a value of $+4|e|$ for the charge on the Sn core. Since the Mg ion charge, $e_2$, was determined by equation (4), $e_1$ was determined by the condition of charge neutrality in a cell

$$e_1 + e_1' + 2e_2 = 0. \tag{7}$$

The results of our calculation were rather insensitive to the value that we picked for the core charge. Finally, we chose $\beta_3 = 0$ for simplicity (it corresponds to a non-central Mg–Mg force) and $\alpha_3 = 0{\cdot}250 \times 10^4$ dyn/cm to give a reasonable fit to the specific heat data. $\alpha_3$ is the central Mg–Mg force constant. The remaining parameters were then evaluated from equations (4), (5) and (6).

## RESULTS OF THE CALCULATIONS

The roots of the secular equation (1) were solved numerically at the 47 points in $\frac{1}{48}$ of the Brillouin zone chosen by KELLERMAN[23] with an IBM 360-50 computer. The reduced specific heat, $Cv/9R$, where $R$ is the universal gas constant, was calculated from the expression

$$\frac{C_v}{9R} = \frac{\sum E\left(\frac{\hbar\omega}{kT}\right) w(q)}{9\sum w(q)},$$

where the sum is over all calculated frequencies, and

$$E(x) = \frac{x^2 e^x}{(e^x - 1)^2}$$

is the reduced Einstein specific heat for a single oscillator of frequency, $\omega$. The weight function $w(q)$ is the number of wave vectors in the entire Brillouin zone equivalent to $q$, where $q$ is one of the 47 points in $\frac{1}{48}$ of the Brillouin zone.

boundary. These low frequencies are responsible for the sharp minimum in the Debye curve near 20°K. The point ion models predicted considerably higher frequencies and did not reproduce the minimum. Low frequency transverse acoustic modes have been found from inelastic neutron scattering measurements in other semiconductors.[18,27,28]

The optic modes were found to be quite flat, and since these frequencies were fitted at $q = 0$,

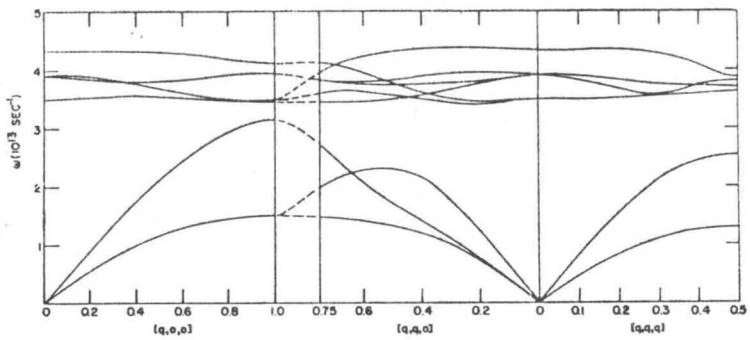


FIG. 7. Phonon dispersion curves for $Mg_2Sn$ calculated from a shell model. The low frequency transverse acoustic modes are responsible for the sharp minimum in the Debye temperature near 20°K.

It is customary to display results of specific heat calculations or measurements in terms of the Debye curve as a function of temperature. In Fig. 5, we have shown the results of our calculations for the shell model and the two point ion models along with the experimental results of JELINEK *et al.*[4] It can be seen that the shell model calculations agreed with experiment better than either point ion model calculations especially at the low temperature minimum in the Debye curve. None of the models agreed particularly well with the experimental curve above 140°K, where the Debye temperature decreases steadily. A similar high temperature decrease can be seen in some alkali halides[22] and III–IV compounds.[15] Generally, such a decrease in $\theta_D$ has been attributed to anharmonic effects, which are not included in a harmonic approximation to lattice dynamics.

The lattice vibration frequencies calculated for the shell model are shown in Fig. 7 for wave vectors, $q$, along the principal symmetry directions. Our results showed that the transverse acoustic modes have very low frequencies, even at the zone

the calculated curves should be reasonably accurate. The Raman modes, however, were not fitted at $q = 0$ since $\omega_R$ was not known; the Raman frequency was sensitive to the Mg–Mg force constant $\alpha_3$. We picked $\alpha_3$ so that the Debye curve agreed with experiment. Decreasing $\alpha_3$, for example, caused a vertical shift downward of the Debye curve below the experimental value and an over-all lowering of the Raman mode frequencies.

## SUMMARY

The elastic properties of $Mg_2Sn$ and the related compounds $Mg_2Si$ and $Mg_2Ge$ are quite similar to those of a number of common semiconductors. An interesting feature of the $Mg_2X$ compounds, however, is the small departure from the condition of elastic isotropy, especially in $Mg_2Si$ and $Mg_2Ge$.

The SZIGETI[25,26] charge, which was the effective ionic charge of the Mg ions in our shell model, was found to be approximately 0·3e for $Mg_2Sn$. (It was also found to be about 0·3e in

$Mg_2Si$ and $Mg_2Ge$.) Such a small charge is consistent with the covalent nature of the bonding in these compounds, yet it is large enough to account for the infrared reflectivity spectrum which is characteristic of an ionic compound.

Calculations of the lattice vibration frequencies in $Mg_2Sn$ could be compared with experiment only by comparing the calculated and experimental Debye curves. Good agreement was attained when the polarizability of the Sn was taken into account. The sharp minimum in the Debye temperature near 20°K was found to be due to a low-lying transverse acoustic mode. Inelastic neutron scattering has revealed such a mode in Ge[18,27] and GaAs.[18,28] More experimental information, such as the Raman spectrum, multiple phonon absorption frequencies, and inelastic neutron scattering, is necessary to provide a more accurate description of the phonons in $Mg_2Sn$, but, the results of the present investigation are thought to give a reasonable first approximation.

*Acknowledgments*—The authors would like to acknowledge the assistance of Mr. H. R. SHANKS in the early part of the experimental work and especially for measuring the thermal expansion coefficient. The authors would also like to thank L. D. CROSSMAN for growing the crystals.

## REFERENCES

1. WHITTEN W. B., CHUNG P. L. and DANIELSON G. C., *J. Phys. Chem. Solids* **26,** 49 (1965).
2. CHUNG P. L., WHITTEN W. B. and DANIELSON G. C., *J. Phys. Chem. Solids* **26,** 1753 (1965).
3. KAHAN A., LIPSON H. G. and LOEWENSTEIN E. V., *Proc. 7th Int. Conf. Phys. of Semicond.*, Paris, 1067 (1964).
4. JELINEK F. J., SHICKELL W. D. and GERSTEIN B. C., *Thermal Study of Group II–IV Semiconductors. II. Heat Capacity of $Mg_2Sn$ In the Range 5–300°K., J. Phys. Chem. Solids* **28,** 267 (1967).
5. MORRIS R. G., REDIN R. D. and DANIELSON G. C., *Phys. Rev.* **109,** 1909 (1958).
6. KOENIG P., LYNCH D. W. and DANIELSON G. C., *J. Phys. Chem. Solids* **20,** 122 (1961).
7. HELLER M. W. and DANIELSON G. C., *J. Phys. Chem. Solids* **23,** 601 (1962).
8. WHITTEN W. B. and DANIELSON G. C., *Proc. 7th Int. Conf. Phys. of Semicond.*, Paris, 537 (1964).
9. CROSSMAN L. D. and TEMPLE P. A., *Bull. Am. Phys. Soc.* **11,** 1121 (1965).
10. WILLIAMS J. and LAMB J., *J. Acoust. Soc. Am.* **30,** 308 (1958).
11. MCSKIMIN H. J., *J. appl. Phys.* **24,** 988 (1953).
12. NBS Circular 539, Vol. V, p. 41.
13. SHANKS H., Private communication.
14. HUNTINGTON H. B., *Solid State Physics* **7,** 218 (1958).
15. WILLARDSON R. K. and BEER A. C., *Semiconductors and Semimetals*, Vol. 2, p. 56, Academic Press, New York (1966).
16. LYDDANE R. H., SACHS R. G. and TELLER E., *Phys. Rev.* **59,** 673 (1941).
17. DICK B. G. and OVERHAUSER A. W., *Phys. Rev.* **112,** 90 (1958).
18. See for example, *Lattice Dynamics, Proc. Int. Conf. Denmark.* Ed. by WALLIS R. F. (1963).
19. MOOSER E. and PEARSON W. B., *J. Electronics* **1,** 629 (1956).
20. BLUNT R. F., FREDERIKSE H. P. R. and HOSLER W. R. *Phys. Rev.* **100,** 663 (1955).
21. LICHTER B. D., *J. electrochem. Soc.* **109,** 819 (1962).
22. KARO A. M. and HARDY J. R., *Phys. Rev.* **129,** 2024 (1963).
23. KELLERMANN E. W., *Phil. Trans. R. Soc.* (London) A**238,** 513 (1940).
24. GANESAN S. and SRINIVASAN R., *Can. J. Phys.* **40,** 74 (1962).
25. SZIGETI B., *Trans. Faraday Soc.* **45,** 1955 (1949).
26. SZIGETI B., *Proc. R. Soc.* A**204,** 51 (1950).
27. BROCKHOUSE B. N. and IYENGAR P. K., *Phys. Rev.* **111,** 74 (1958).
28. DOLLING G. and WAUGH J. L. T., *Lattice Dynamics, op. cit.*, p. 19.

## APPENDIX

Following GANESAN and SRINIVASAN[24] we define the matrix of force constants between one ion and another. The matrix can be written most generally as

$$D = \begin{pmatrix} \phi_{xx} & \phi_{xy} & \phi_{xz} \\ \phi_{yx} & \phi_{yy} & \phi_{yz} \\ \phi_{zx} & \phi_{zy} & \phi_{zz} \end{pmatrix}$$

where, for example, $\phi_{xy} = (\partial^2\phi/\partial x\partial y)$ is evaluated at the equilibrium separation. $\phi$ is the two-body potential associated with the short range forces between one ion and another.

We list the matrix of force constants for the Sn core–Sn shell, nearest neighbor Mg–Sn, next nearest

neighbor Sn–Sn and Mg–Mg interactions. The requirements of symmetry greatly reduce the number of independent constants.

$$D^{\text{Sn core- Sn Shell}} = \begin{pmatrix} \delta & 0 & 0 \\ 0 & \delta & 0 \\ 0 & 0 & \delta \end{pmatrix}$$

$$D^{\text{Mg-Sn}} = \begin{pmatrix} \alpha_1 & \beta_1 & \beta_1 \\ \beta_1 & \alpha_1 & \beta_1 \\ \beta_1 & \beta_1 & \alpha_1 \end{pmatrix}$$

$$D^{\text{Sn-Sn}} = \begin{pmatrix} \alpha_2 & 0 & 0 \\ 0 & \beta_2 & \gamma_2 \\ 0 & \gamma_2 & \beta_2 \end{pmatrix},$$

$$D^{\text{Mg-Mg}} = \begin{pmatrix} \beta_3 & 0 & 0 \\ 0 & \beta_3 & 0 \\ 0 & 0 & \alpha_3 \end{pmatrix}.$$